






## RESEARCH ARTICLE

10.1029/2022MS003277

# Global Mapping of Potential and Climatic Plant-Available Soil Water

 Surya Gupta<sup>1,2</sup> , Peter Lehmann<sup>1</sup> , Samuel Bickel<sup>1,3</sup>, Sara Bonetti<sup>4</sup>, and Dani Or<sup>1,5</sup> 

<sup>1</sup>Soil and Terrestrial Environmental Physics, ETH, Zürich, Switzerland, <sup>2</sup>Department of Environmental Sciences, University of Basel, Basel, Switzerland, <sup>3</sup>Institute of Environmental Biotechnology, Graz University of Technology, Graz, Austria, <sup>4</sup>Laboratory of Catchment Hydrology and Geomorphology, School of Architecture, Civil and Environmental Engineering, EPFL Valais Wallis, Sion, Switzerland, <sup>5</sup>Department of Civil and Environmental Engineering, University of Nevada, Reno, Reno, NV, USA

**Key Points:**

- Global maps of field capacity (FC) are compared based on dynamic and static definitions
- Local climate effects of evaporation and rainfall frequency via dynamic FC affect climatic plant-available soil water (PASW)
- Incorporating climatic effects mainly reduces PASW in arid regions compared to humid climates

**Supporting Information:**

Supporting Information may be found in the online version of this article.

**Correspondence to:**

S. Gupta,  
[surya.gupta@unibas.ch](mailto:surya.gupta@unibas.ch)

**Citation:**

Gupta, S., Lehmann, P., Bickel, S., Bonetti, S., & Or, D. (2023). Global mapping of potential and climatic plant-available soil water. *Journal of Advances in Modeling Earth Systems*, 15, e2022MS003277. <https://doi.org/10.1029/2022MS003277>

Received 5 AUG 2022  
Accepted 21 OCT 2023

**Abstract** The estimation of plant-available soil water (PASW) is essential to quantify transpiration fluxes, the onset of heatwaves, irrigation water management, land-use decisions, vegetation ecology, and land surface memory in climate models. PASW is the amount of stored water available for plant use. It is broadly defined as the difference between soil water content at field capacity (FC) and wilting point (WP) in the root zone. The limiting states of FC and WP are linked to gravitational drainage and plant physiology and are often deduced from soil water characteristics at prescribed matric potentials (−3.3 and −150 m for FC and WP, respectively). Evidence suggests that static definition of FC at a constant matric potential ignores dynamic effects on FC attainment affected by soil and climate. Here, we revise the definition of PASW by considering (a) soil-specific dynamic effects and (b) local climate effects of evaporation and rainfall frequency on PASW. The new global PASW maps benefit from state-of-the-art soil maps, water characteristic parameterization, and incorporation of dynamic definition of FC. For completeness we provide static and dynamic PASW estimates. Globally, ice-free soils store up to 19,941 km<sup>3</sup> of water in the top 1 m (representing 18% of annual terrestrial precipitation). Adjusted for local climatic conditions, global PASW storage rarely exceeds 14,853 km<sup>3</sup> per year highlighting the need for multiple refilling of soil profiles. Differences between potential and climatic PASW are manifested primarily in arid regions (where soil profiles are rarely filled to capacity) whereas in humid regions differences in PASW storage are minor.

**Plain Language Summary** Plant-available soil water (PASW) is defined as the amount of water held in soil that can be used by plants. It is conventionally estimated as the difference between field capacity (FC) and wilting point (WP), which depend on soil type and plant physiology. Water contents at FC and WP are usually deduced at fixed matric potentials irrespective of soil types (−3.3 and −150 m for FC and WP, respectively). However, FC is affected by various factors such as soil texture, soil structure, and clay type that affect the dynamics of FC attainment and put into question the use of a static definition based on constant matric potentials. Therefore, we used the approach developed by Assouline and Or (2014, <https://doi.org/10.1002/2014wr015475>) that considers a dynamic definition of FC based on soil-specific matric potential values beyond which the soil water continuity is substantially reduced or disrupted. The potential PASW was calculated by subtracting the WP from the dynamic FC. The novelty of this study is to incorporate the effect of climate such as evaporative water loss to introduce a climatic PASW. Our results suggest that PASW in arid regions are overestimated when climatic effects are ignored.

## 1. Introduction

Plant-available soil water (PASW) is a key determinant of the potential yield of crops in agroecosystems and modulates natural vegetation productivity. Traditionally, PASW has been used for crop management as it provides information useful for scheduling irrigation, time of sowing, as well as other agronomic inputs (e.g., fertilizer application) (Lamm et al., 1994). Additionally, PASW is used to estimate vegetation carrying capacity and dynamics in Earth system models (Silva et al., 2014; Wheeler & Read, 2016). Soil acts as a leaky reservoir of water for plants, requiring a practical definition of how much soil water holding capacity is available for plant use. The term PASW was proposed by Veihmeyer and Hendrickson (1931) and Veihmeyer and Hendrickson (1949) and defines the soil water content between field capacity (FC) and wilting point (WP). The value of WP is generally set equal to a water content at −150 m. At such negative water potential values, the soil water characteristic

© 2023 The Authors. Journal of Advances in Modeling Earth Systems published by Wiley Periodicals LLC on behalf of American Geophysical Union. This is an open access article under the terms of the Creative Commons Attribution-NonCommercial-NoDerivs License, which permits use and distribution in any medium, provided the original work is properly cited, the use is non-commercial and no modifications or adaptations are made.

curves (SWCCs) become flat and the quantification of PASW is less affected by uncertainties of matric potential values for WP compared to FC. Compared to the definition of the WP, the quantification of the FC is more ambiguous as we discuss in the next paragraph.

It has been observed that in many soils, the attainment of FC is associated with matric potential values close to  $-3.3$  m; this value has been proposed by Colman (1947) as a practical definition for FC and was adopted by the community (Mantovanelli et al., 2021; Minasny & McBratney, 2018). This definition was adjusted to  $-1$  m for sandy soils due to rapid drainage and a sharp drop in hydraulic conductivity at low matric potentials (Dahiya et al., 1988; Robertson et al., 2021).

Assouline and Or (2014) have addressed the dynamics of FC attainment as the state at which hydraulic continuity for internal drainage is significantly reduced or disrupted. This state is related to a soil-specific capillary pressure that limits the continuity of capillary flow as proposed by Lehmann et al. (2008) for evaporation and applied by Assouline and Or (2014) for cessation of internal drainage. This approach provides a consistent definition of FC attainment across soils as evaluated by Assouline and Or (2014) and more recently by Asadi et al. (2020). We will use this definition of FC to calculate the amount of PASW.

Despite its usefulness and applications in the agronomic context, the concept of FC remains a subject of controversy due to its dual definition (a static one based on matric potential and a dynamic one based on rates of internal drainage) and the limited consideration of natural vegetation with mixed rooting zones and traits (Assouline & Or, 2014; de Jong van Lier & Wendroth, 2016; Jabro et al., 2009; Logsdon, 2019). The various factors affecting FC such as soil texture, soil structure, clay type, soil layering and depth to groundwater (Hillel, 2012; Kirkham, 2005; Ottoni Filho et al., 2014) limit the relevance of a static definition based on prescribed matric potential. For example, Jabro et al. (2009) estimated FC for sandy loam and clay loam soils based on the attainment of constant pressure following redistribution of infiltration water. Convergence to equilibrium conditions was achieved approximately after 50 and 450 hr reaching matric potentials of 1.8 and 2.7 m for sandy loam and clay loam, respectively. Similarly, de Jong van Lier and Wendroth (2016) estimated FC through numerical simulations of internal drainage based on the attainment of internal drainage rates that are smaller than evaporation rates. Likewise, Twarakavi et al. (2009) used a flux-based definition of FC and developed an analytical expression to reproduce the results of numerical experiments.

The traditional definition of PASW (using either static or dynamic FC) focuses on the capacity of the leaky reservoir (soil) to hold plant useable soil water. In many biomes, climatic conditions constrain the refilling of this potential PASW storage reservoir. We seek to introduce a climate-informed representation of PASW that considers not only soil capacity but also local climatic conditions such as rainfall distribution and evaporation that removes water from the reservoir (see Figure 1). This derived variable (termed climatic PASW (cPASW)) departs from the agronomic PASW concept and reflects the climatic water reservoir available to natural vegetation in different biomes. In this study, we denote traditional PASW as potential PASW (pPASW) in contrast to the cPASW, which considers climatic constraints. We base the derivation of cPASW on Bickel and Or (2020) that proposed a procedure for estimating climatic water content using average precipitation frequency and evaporation dynamics (see Section 2.5).

Regardless of whether a static or a dynamic definition of FC is sought, the assessment of PASW requires knowledge of SWCC information in terms of a parametric model. The approach of Assouline and Or (2014) is based on the SWCC model of van Genuchten (1980) that requires four parameters, namely shape parameters  $\alpha$  (1/m) and  $n$  (dimensionless), saturated water content  $\theta_s$  ( $\text{m}^3/\text{m}^3$ ), and residual water content  $\theta_r$  ( $\text{m}^3/\text{m}^3$ ). Pedotransfer functions (PTFs) have often been used to map these parameters at the global scale (Dai et al., 2019; Simons et al., 2020; Zhang & Schaap, 2017) using information on basic soil properties (soil texture, bulk density, and organic content). However, such PTF-based maps are developed using samples mainly collected from agricultural land in temperate regions and do not represent the variance of soil formation processes for other land use and climatic zones (Gupta et al., 2021; Or, 2020). To overcome these limitations, Gupta et al. (2022a) developed an improved global map of van Genuchten (vG) parameters that considered the effect of soil forming factors (vegetation, climate, and topography) based on measured SWCCs from all continents. The objective of this study are (a) to use the modified vG parameters estimated by Gupta et al. (2022a) to compute FC maps using the approach of Assouline and Or (2014) and (b) to link pPASW with climatic average water storage (Bickel & Or, 2020) to develop a cPASW map.

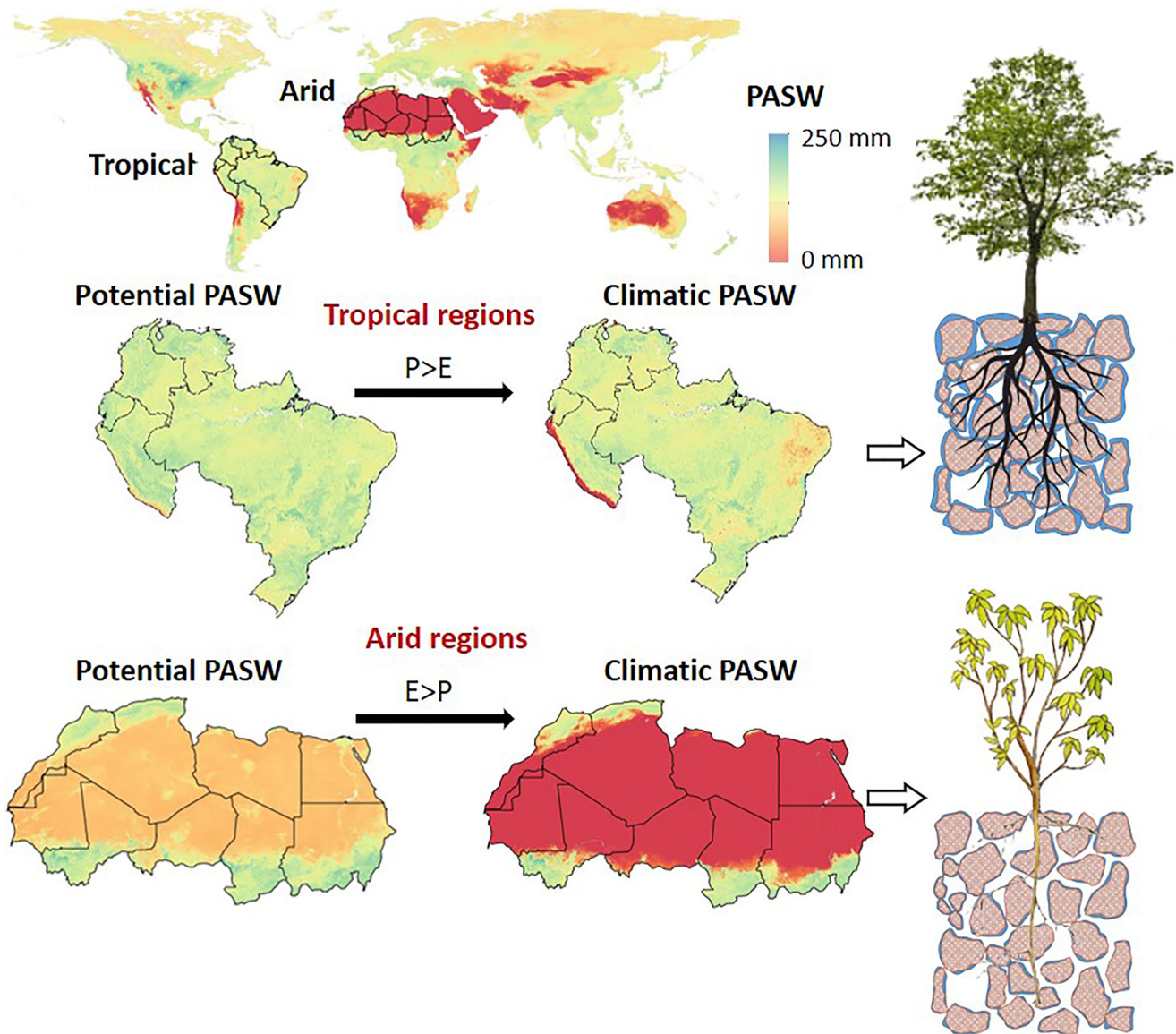


**Figure 1.** Conceptual diagram showing the difference between the potential plant-available soil water (pPASW) and climatic PASW (cPASW). In tropical regions (e.g., the Amazon basin region), the frequency and amount of precipitation ( $P$ ) are higher than the water loss due to evapotranspiration ( $E$ ). The plant-available water equals the potential amount defined by field capacity ( $FC$ ) and wilting point. On the other hand, in arid regions (e.g., the Sahara region and the Peruvian coastal desert shown in the upper panel), the cPASW is significantly lower than the pPASW due to limited precipitation and high evaporative losses such that pPASW is never realized (i.e., the water content after rainfall is smaller than  $FC$ ). The map at the top shows the main outcome of this study, with cPASW expressed in mm water per meter soil depth (cPASWD1m). Because we express PASW in units of water content, water depth per area or water volume, we refer to the notation at the end of the article.

## 2. Material and Methods

### 2.1. Soil Water Content at Field Capacity ( $FC$ )

For the parameterization of soil  $FC$ , we employ two approaches—standard definition (water content at  $-3.3$  m capillary pressure head) and the estimation of  $FC$  based on Assouline and Or (2014) using a critical water content that marks the disruption of hydraulic connectivity and thus cessation of internal drainage. The standard definition of  $FC$  is stated as the amount of water remaining in soil two or three days after wetting (SSSA, 2008). However, in practice, a value of  $FC$  equal to the water content at  $-3.3$  m is often used as a means of standardization (Mantovanelli et al., 2021; Minasny & McBratney, 2018). In contrast, Assouline and Or (2014) defined  $FC$  at a

critical capillary pressure below which the continuity of capillary flow paths is limited (Lehmann et al., 2008). This intrinsic capillary pressure value  $\psi_{FC}$  is given by:

$$\psi_{FC} = \frac{1}{\alpha} \left( \frac{n-1}{n} \right)^{\frac{1-2n}{n}} \quad (1)$$

where  $\alpha$  ( $\text{m}^{-1}$ ) and  $n$  (dimensionless) are soil parameters in the vG expression. This may be expressed in terms of effective soil saturation  $S_{FC}$ :

$$S_{FC} = S(\psi_{FC}) = \left( \frac{\theta_{FC} - \theta_r}{\theta_s - \theta_r} \right) = \left[ 1 + (\alpha |\psi_{FC}|)^n \right]^{\frac{1-n}{n}} \quad (2)$$

where  $\theta_s$  and  $\theta_r$  are the saturated and residual soil water content ( $\text{m}^3/\text{m}^3$ ), respectively, and  $\theta_{FC}$  is the water content at FC that is related to  $\psi_{FC}$  using the SWCC. The corresponding water content  $\theta_{FC}$  is obtained from Equation 2, and the unsaturated hydraulic conductivity  $K(S_{FC})$  is based on the model of Mualem (1976), given by:

$$K(S_{FC}) = K_s S_{FC}^{0.5} \left[ 1 - \left( 1 - S_{FC}^{(1/m)} \right)^m \right]^2 \quad (3)$$

where  $m = 1 - 1/n$ .

The amount of drainable water from the soil profile of depth  $z$  at FC,  $Q_{FC}$ , is then calculated as:

$$Q_{FC} = z(\theta_s - \theta_{FC}). \quad (4)$$

Assouline and Or (2014) also proposed a dynamic criterion for the attainment of FC. Gravity is the primary driving force affecting water flow during drainage and the hydraulic gradient reaches unity near FC (Zacharias & Bohne, 2008). This implies that the water flux ( $q_{FC}$ ) at a given depth  $z$  is equal to the corresponding unsaturated hydraulic conductivity ( $K_{FC}$ ):

$$q_{FC} = K(S_{FC}). \quad (5)$$

Consequently, a characteristic time for the attainment of FC,  $\tau_{FC}$ , can be deduced from the ratio of amount between drainable water ( $Q_{FC}$ ) and the water flux ( $q_{FC}$ ):

$$\tau_{FC} = \frac{Q_{FC}}{q_{FC}} \quad (6)$$

This characteristic time  $\tau_{FC}$  is computed based on the drainage rate when the soil is at its FC ( $q_{FC} = K(S_{FC})$ ). The drainage rate from wet soil is initially much higher. By computing an effective conductivity for the entire drainage period, Assouline and Or (2014) could show that the absolute time to reach FC,  $T_{FC}$ , equals:

$$T_{FC} = 0.092\tau_{FC} \quad (7)$$

## 2.2. Input Data Sets

We use novel global maps of vG soil water retention model (vG) parameters ( $\alpha$ ,  $n$ ,  $\theta_s$ , and  $\theta_r$ ) at different depths (0, 30, 60, and 100 cm) with spatial resolution of 1 km developed by Gupta et al. (2022a) and the map of saturated hydraulic conductivity ( $K_{sat}$ ) from Gupta et al. (2021). These maps were developed using Covariate-based GeoTransfer Functions that included local covariates such as climate, terrain, and vegetation metrics in the prediction of soil hydraulic properties. For the determination of the climatic water content (Section 2.5), the number of consecutive days (Bickel & Or, 2021) without rainfall was determined using multi-source weighted ensemble precipitation (MSWEP, Beck et al., 2019) with precipitation records of 37 years (1979–2016) at a daily resolution. The MSWEP data was originally obtained at 3-hourly temporal resolution and  $0.1^\circ$  spatial resolution. The data were further aggregated to a daily temporal resolution to use in this study. The potential evaporation was calculated based on the approach by Jensen and Haise (1963) using WorldClim (Fick & Hijmans, 2017) mean annual radiation and temperature as inputs (for more information see Text S1 in Supporting Information S1).



### 2.3. Comparison of FC Maps Produced by Standard and Dynamic Approaches

Definitions of FC were compared using point data (11,705 SWCCs with fitted vG parameters) from Gupta et al. (2022b). Values of  $\theta_{FC}$  as defined by the cessation of capillary flow were computed using Equation 2 for all SWCCs. For 1,288 SWCCs the water content was measured at  $-3.3$  m and could be compared with the results of Equation 2. Similarly, the global map of vG parameters was used to compute global maps of  $\theta_{FC}$  based on the approach from Assouline and Or (2014) for comparison with FC maps using the standard approach (water content at  $-3.3$  m pressure head). We used FC maps based on the standard approach from (a) Gupta et al. (2022a) including environmental covariates, and (b) Zhang et al. (2018) that computed FC based on a PTF predicting parameter values of the Kosugi water retention model (Kosugi, 1994). Zhang et al. (2018) produced maps that are highly cited and used by the research community. Moreover, the authors considered the FC at  $-3.3$  m. Therefore, it was interesting to compare our approach with their method.

### 2.4. Estimation of pPASW Map

We calculated the FC capillary pressure head  $\psi_{FC}$  based on Equation 1 and the corresponding water content (Equation 2) for different depths (0, 30, 60, and 100 cm) and we used vertical averaging to estimate FC over 1 m. We assumed the WP at the matric potential of  $-150$  m. Then, we subtracted the averaged water content at  $-150$  m matric potential ( $\theta_{WP}$ ) from the FC water content to obtain the pPASW map (PASW expressed as volumetric water content) and multiplied by the soil depth ( $z = 1$  m) to obtain the height of PASW in the first meter of soil, pPASWD1m (see Figure 2),

$$\text{pPASWD1m} = z \cdot (\theta_{FC} - \theta_{WP}). \quad (8)$$

The pPASWD1m map produced in this study was compared with the widely used PASWC map by Zhang et al. (2018), who produced the map by subtracting the FC ( $-3.3$  m) and permanent WP. We multiplied the Zhang et al. (2018) PASWC map by the soil depth ( $z = 1$  m) to allow the comparison.

### 2.5. Calculation of Climatic Water Content (CWC) and cPASW

The climatic averaged PASW is defined by considering the available local precipitation record and adjusting for local evaporative losses. The cPASW of each pixel of the globe was calculated based on four steps (see as well Figure 2). In the first step, the time  $T_{FC}$  to drain a soil profile of 1 m depth from saturation to FC was calculated based on Equation 7 using depth averaged hydraulic properties. In a second step, we used rainfall data to determine the average number of consecutive dry days  $T_{dry}$  between rainfall events. The MSWEP data set has a spatial resolution of  $0.1^\circ$  and we resampled  $T_{dry}$  to  $0.01^\circ$  (approximately 1 km at equator) using nearest neighbor interpolation. By comparing  $T_{dry}$  with  $T_{FC}$ , we can distinguish regions with  $T_{dry} > T_{FC}$  where climatic average soil water content conditions are below FC, from regions with  $T_{dry} < T_{FC}$  where the water content often exceeds FC after a dry period. The difference between  $T_{FC}$  and  $T_{dry}$  was calculated to estimate the days for which the evaporation loss was considered. As shown in Figure S1 of the Supporting Information S1, we introduced a temporal index for climatic average time to reach (or fall below) FC. For all sites with  $T_{dry} > T_{FC}$ , the water content dropped below FC to a value  $\theta_{clim}$  defined as climatic water content (see Figure 2) (Bickel & Or, 2020):

$$\theta_{clim} = (\theta_{FC} - \theta_r) \cdot e^{-\frac{E_0}{z \cdot (\theta_{FC} - \theta_r)} (T_{FC} - T_{dry})} + \theta_r \quad (9)$$

with the potential evaporation rate  $E_0$  (m/day) and soil depth ( $z$ ) equal to 1 m. Finally, the climatic PASW (cPASWD1m) for a soil depth of 1 m was calculated as:

$$\text{cPASWD1m} = \begin{cases} z \cdot (\theta_{FC} - \theta_{WP}) & \text{for } T_{dry} < T_{FC} \\ z \cdot (\theta_{clim} - \theta_{WP}) & \text{for } T_{dry} > T_{FC} \end{cases} \quad (10)$$

Climatic water content can be larger than water content at FC (see Figure S1 in Supporting Information S1), however, the values were truncated to FC water content to illustrate the climatic effect for the quantification of PASW. Also, we noticed that the CWC is lower than the WP for certain parts of the arid region, therefore, we assigned a zero value to those regions. After the estimation of potential and cPASW with soil depth  $z$  of 1 m (pPASWD1m and cPASWD1m), the volume of water stored in the top 1 m (PASWV1m) was calculated as:

$$\text{pPASWV1m} = \text{pPASWD1m} \cdot A \quad (11)$$

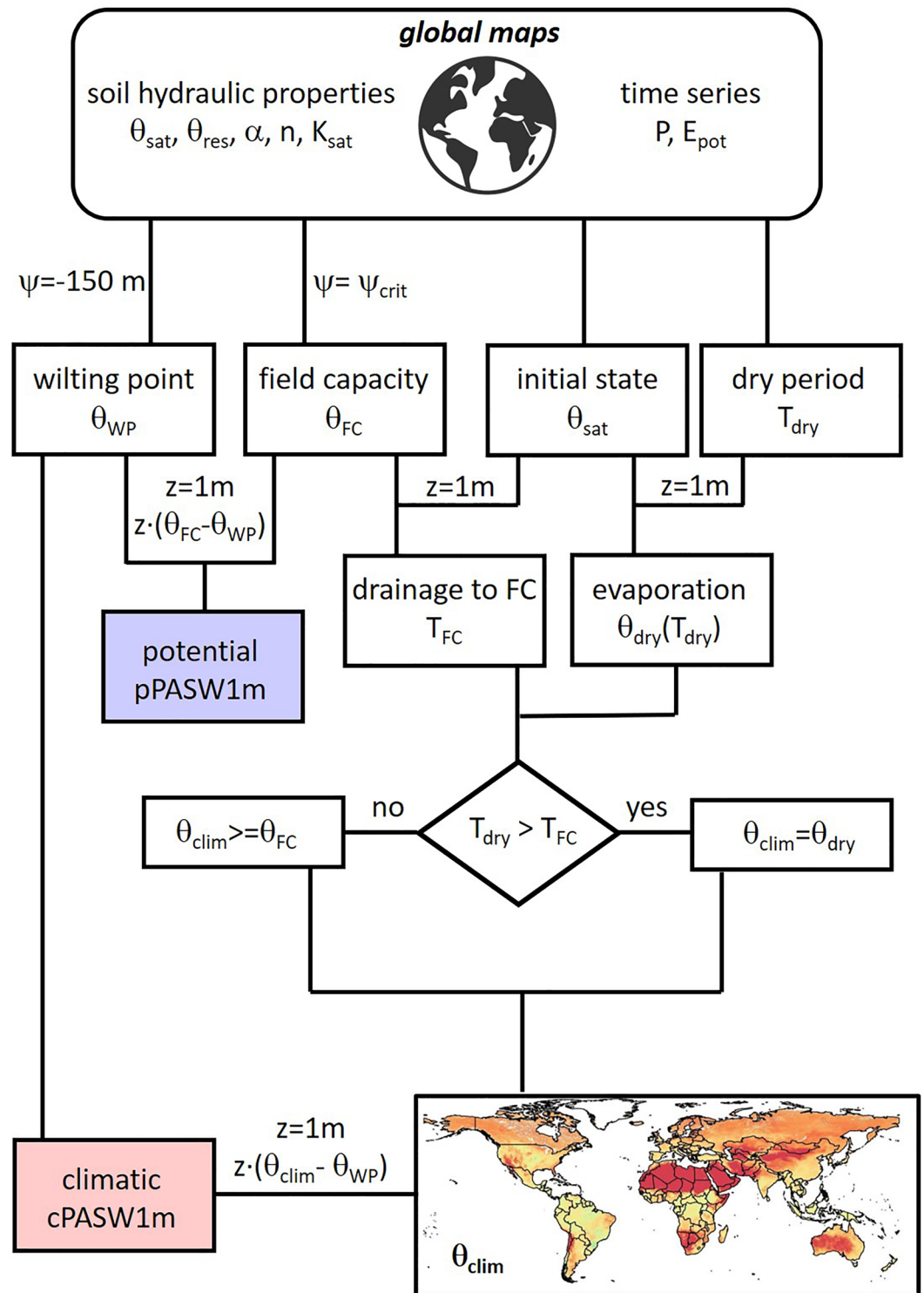


**Figure 2.** Conceptual workflow to describe the estimation of pPASW and climatic PASW for 1 m soil depth. As described in more detail in the text, the potential plant-available soil water (PASW) within a soil layer of 1 m thickness is computed as the difference between field capacity (FC) and wilting point (deduced from the soil water characteristics curve). To determine the climatic water content, the time for drainage by gravity to FC ( $T_{FC}$ ) is compared to the average length of the period of evaporative drying ( $T_{dry}$ ). Note that climatic water content can be larger than water content at FC, however, the values were truncated to FC water content to calculate the PASW affected by the climate.

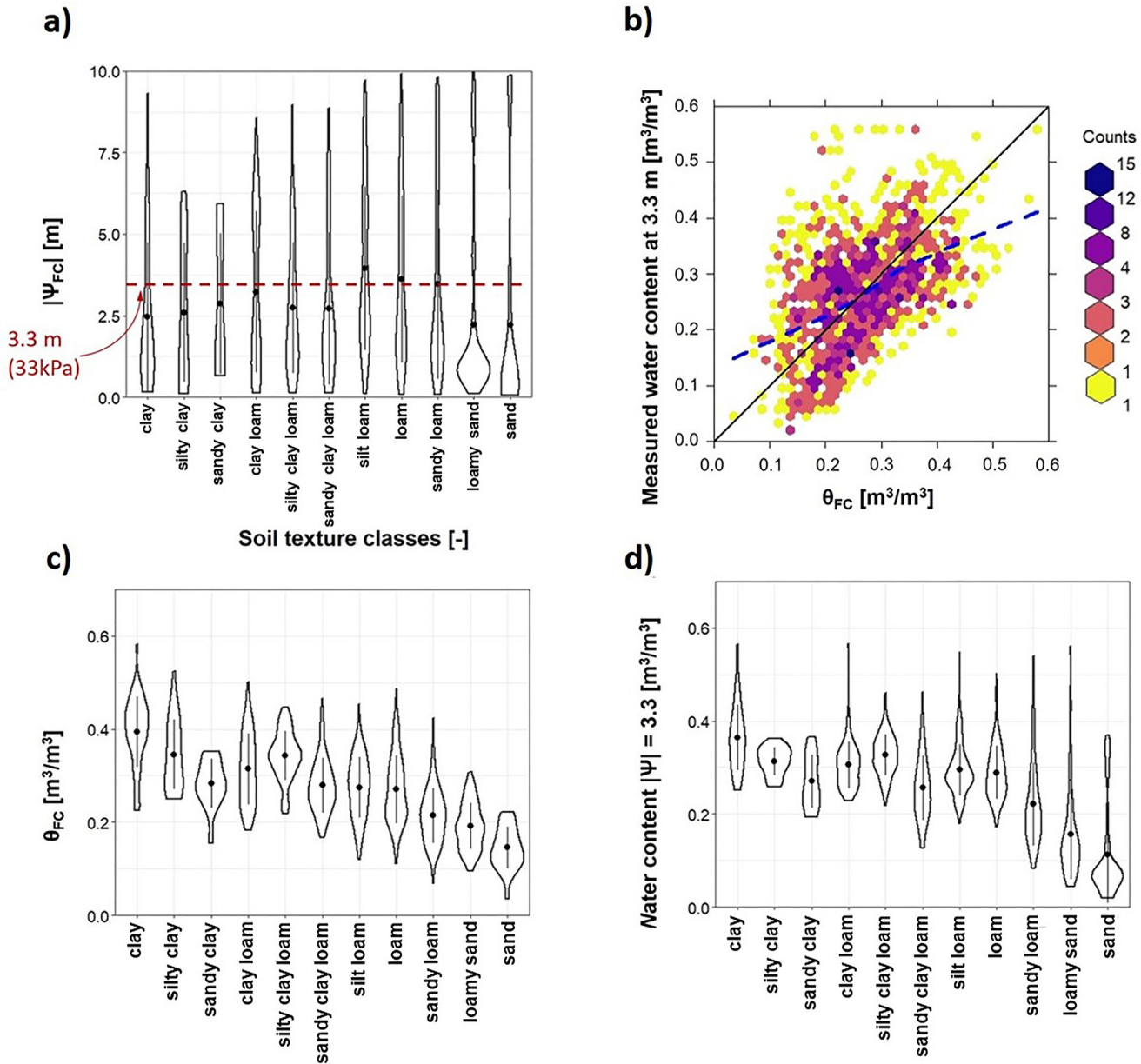


**Figure 3.** (a) Distribution of critical capillary pressure head at field capacity (FC)  $\psi_{FC}$  based on Assouline and Or (2014) approach for each soil textural class with the red dashed line marking the standard definition of FC ( $-3.3$  m). (b) Relationship between water content based on Assouline and Or (2014) and the standard approach (measured water content at  $-3.3$  m), (c) water content at FC ( $\theta_{FC}$ ) using Equation 2, and (d) measured water content at  $-3.3$  m, for each soil textural class. A total of 1,288 curves out of 11,705 fitted soil water characteristic curves in Gupta et al. (2022b) have information on matric potential  $-3.3$  m and are used to produce these figures (a–d).

$$cPASWD1m = cPASWD1m \cdot A \quad (12)$$

where  $A$  is the area of the grid cell (1 square km in this study).

### 3. Results

#### 3.1. Soil Water Regime at FC: Static Criteria

Figure 3a shows the estimated  $\psi_{FC}$  using Equation 1. The mean value of  $\psi_{FC}$  for most of the soil texture classes is typically less negative than the standard FC at constant value of pressure head  $-3.3$  m except for silt loam soil texture class

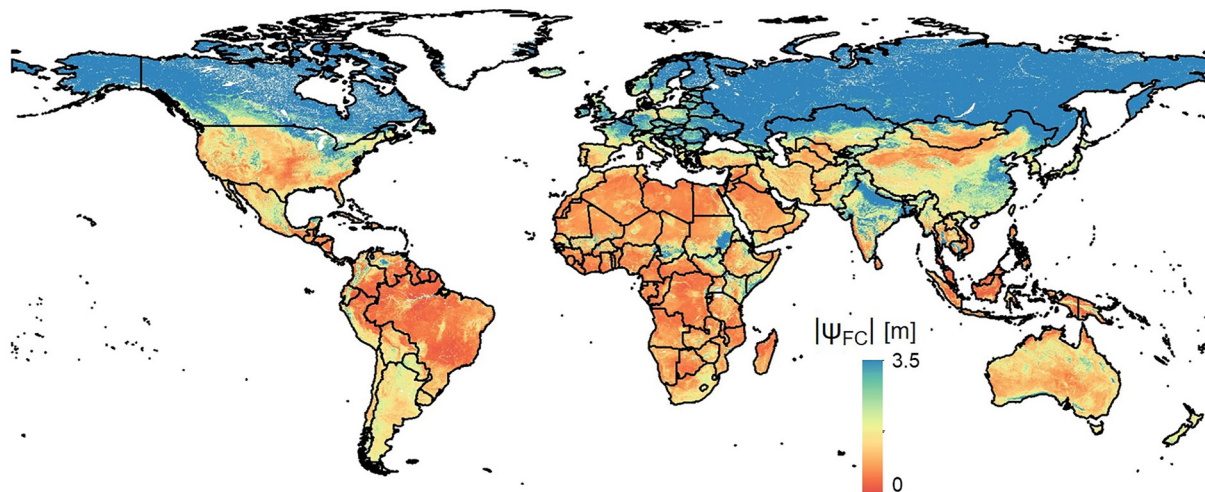


**Figure 4.** Spatial distribution of matric potential at field capacity ( $\psi_{FC}$ ) estimated using the Assouline and Or (2014) approach. Note that the values are truncated to 3.5 m and show the absolute values.

(for loam and sandy loam,  $\psi_{FC}$  mean value is approximately equal to standard FC). Furthermore, Equation 2 is used to calculate  $\theta_{FC}$  as shown in Figure 3b. The trend with soil texture is similar to the standard approach, with slightly lower values when the  $-3.3$  m water content is used as shown in Figures 3b–3d. The global maps of vG parameters are used to calculate the spatial distribution of  $\psi_{FC}$  as shown in Figure 4. The map of  $\psi_{FC}$  illustrates the low absolute values (compared to the classical definition of  $-3.3$  m) on the whole globe except for the higher northern latitudes.

### 3.2. Soil Water Regime at FC: Dynamic Criteria

We further calculated the time required to attain FC ( $T_{FC}$ ) at different depths. We used Equations 4–7 to calculate  $Q_{FC}$ ,  $q_{FC}$ ,  $\tau_{FC}$ , and  $T_{FC}$  respectively. Figure 5a shows the time needed to attain FC from saturation at 1 m soil depth. It shows areas (Central India, Horn of Africa, and Midwest USA) with smectite clay minerals (high water retention areas) that need more time to attain FC while the zones with high sand content (deserts) need less time to attain FC. In Figure 5b, the climatic average soil water content is always below FC ( $T_{dry} > T_{FC}$ ) in arid regions, in contrast to humid climate that often exceed FC ( $T_{dry} < T_{FC}$ ). To show gradual changes between wet and dry regions, we introduce a temporal index (see Figure S1 in Supporting Information S1) and scale the time according to  $(T_{FC} - T_{dry})/T_{dry}$  for dry and  $(T_{FC} - T_{dry})/T_{FC}$  for wet regions to values between  $-1$  and  $1$ .

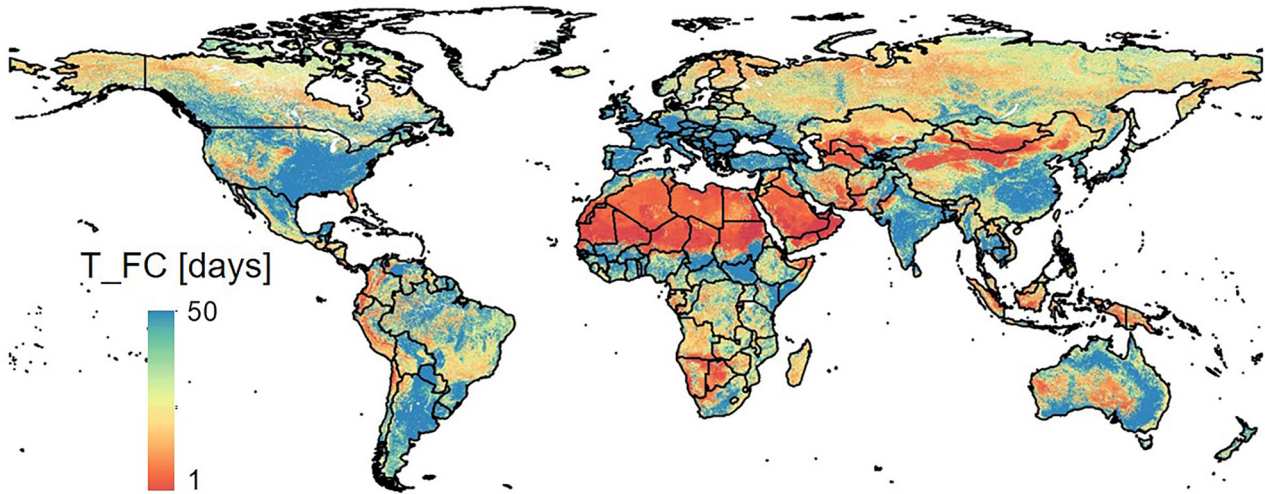
### 3.3. Visual Comparison of FC Maps and Climatic Water Content

The global map of FC produced using Equation 2 is also compared with FC maps based on constant capillary pressure ( $-3.3$  m) as shown in Figure 6. The first difference between the maps is the definition of FC (using Equation 2 or  $-3.3$  m head) and the second difference is with respect to the parameterization of SWCC (vG model for the map (b) of Gupta et al. (2022a) and Kosugi-model for the map (c) of Zhang et al. (2018)). As expected from the analysis presented in Figure 4 ( $\psi_{FC}$  is less negative than  $-3.3$  m), the water content based on Equation 2 presented in Figure 6a is larger in most regions compared to the standard approach ( $-3.3$  m head) shown in Figure 6b. Only in silty and loamy soils of northern latitudes, FC values are higher based on the standard approach. The same regions show high FC values as well for the map (Figure 6c) of Zhang et al. (2018). Due to the dominant effect of high bulk densities in northern latitudes in the underlying PTFs, the FC values are very high. We also notice that FC values for the new map in South America are similar to FC values of Zhang et al. (2018). However, the matric potential to attain FC is more negative in the new map compared to the  $-3.3$  m matric potential.

Likewise, Figure S2a in Supporting Information S1 depicts the global map of climatic water content which represents the availability of water content in soils after the reduction of losses due to evaporation. It shows that regions with high sand content or arid climates are severely affected by evaporation and the PASW is significantly reduced compared to FC (Figure S2b in Supporting Information S1). Table 1 shows that after applying the climatic effect, 37% of potential FC was reduced for arid regions. On the other hand, higher northern latitudes and tropical regions are the least affected regions (cPASWD1m close to pPASWD1m).



a) Days to FC at 1 m



b) Regions attaining climatic FC

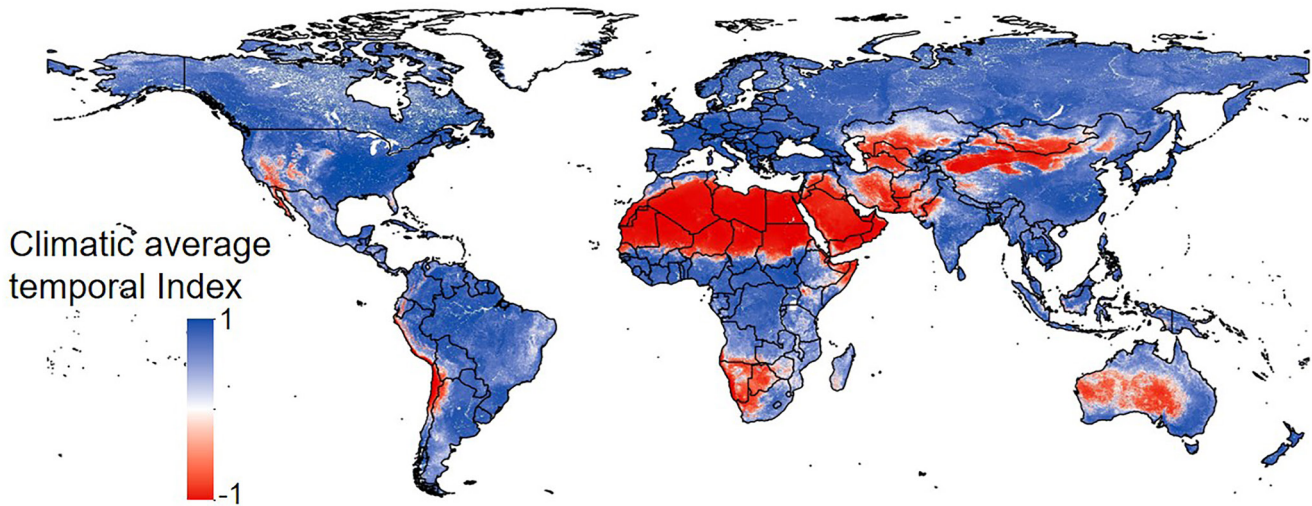
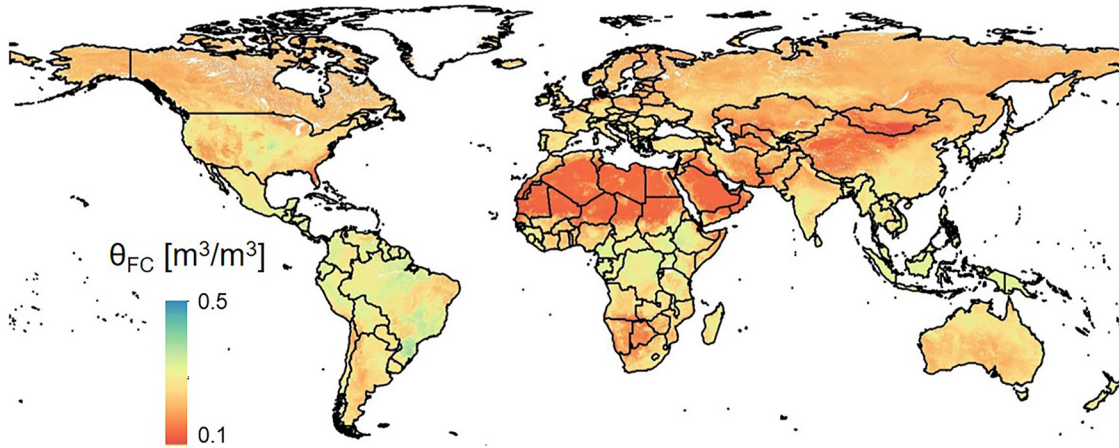


**Figure 5.** Global maps of rates and time to attain field capacity (FC) from saturation at 1 m depth. (b) Classification of geographic regions where climatic average soil water content conditions are below FC (red) or exceed FC (blue) expressed as temporal index values in the range of +1 (blue), 0 (white) and -1 (red) as illustrated in Figure S1 of the Supporting Information S1.

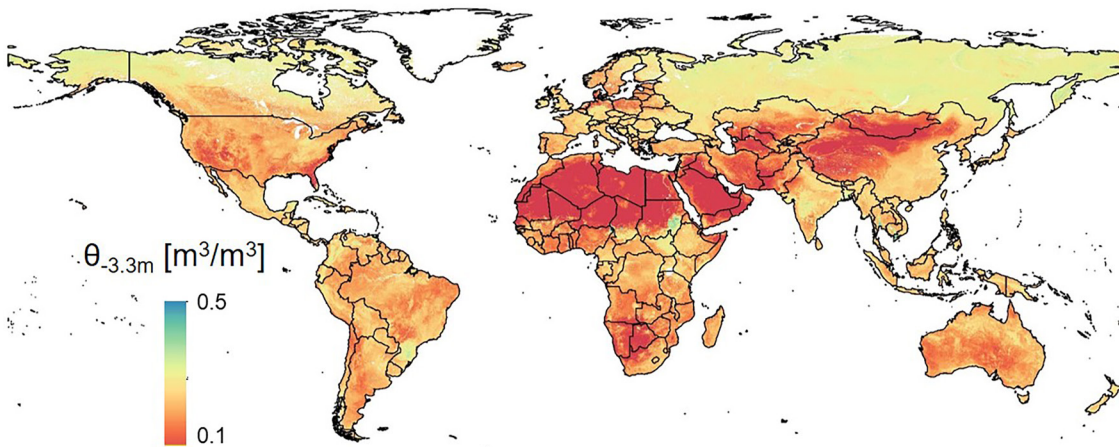
### 3.4. Global Distribution of Plant-Available Soil Water

Figure 7a shows the global map of PASW that is calculated using the maps of  $\theta_{FC}$  and  $\theta_{WP}$  for 1 m soil depth (pPASWD1m). Our map shows that the values are higher in desert regions than in the map of Zhang et al. (2018) (Figure 7b). Moreover, our map provides higher values in the tropical regions, central parts of India, the eastern parts of the USA, and parts of China, as compared to Zhang et al. (2018) PASW map (see Figure S3 in Supporting Information S1). In contrast, Zhang et al. (2018) provide high values for higher northern latitudes. Figure 8a shows the climatic PASW for 1 m depth (cPASWD1m) based on Equation 10, which displays a lower water availability in desert regions compared to pPASWD1m (Figure 7a). The main difference between the two maps is the low water availability in the desert regions of the cPASW map as compared to the pPASW map. Other regions are less affected compared to desert regions. The mean pPASWD1m is reduced from 144 to 107 mm after incorporating the climatic effects (Figure 8b). Similarly, the capacity to store water against gravity in the top 1 m of ice-free soils is decreased from 19,941 km<sup>3</sup> (pPASWV1m) to 14,853 km<sup>3</sup> (cPASWV1m) globally.

a)  $\theta_{FC}$



b)  $\theta_{FC_{-3.3\ m}}$



c) Zhang et al., 2018

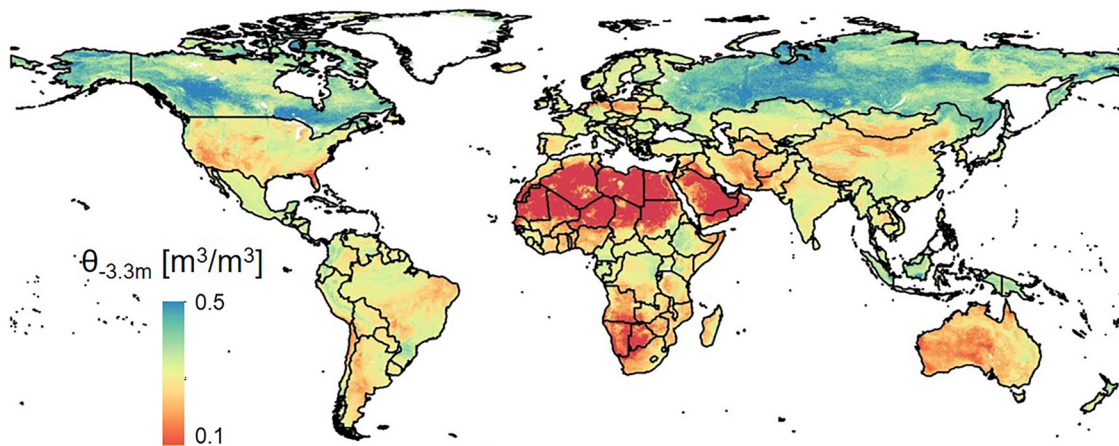


**Figure 6.** Comparison of the global distribution of water content at field capacity (FC) (a) based on Assouline and Or (2014) with (b) the map of water content at  $-3.3$  m matric potential produced using van Genuchten parameters from Gupta et al. (2022a), and with (c) the map of Zhang et al. (2018). In contrast to (a), FC maps (b) and (c) are based on constant matric potential ( $-3.3$  m).



**Table 1**  
Average Values of Field Capacity and Plant-Available Soil Water Among Different Climatic Regions

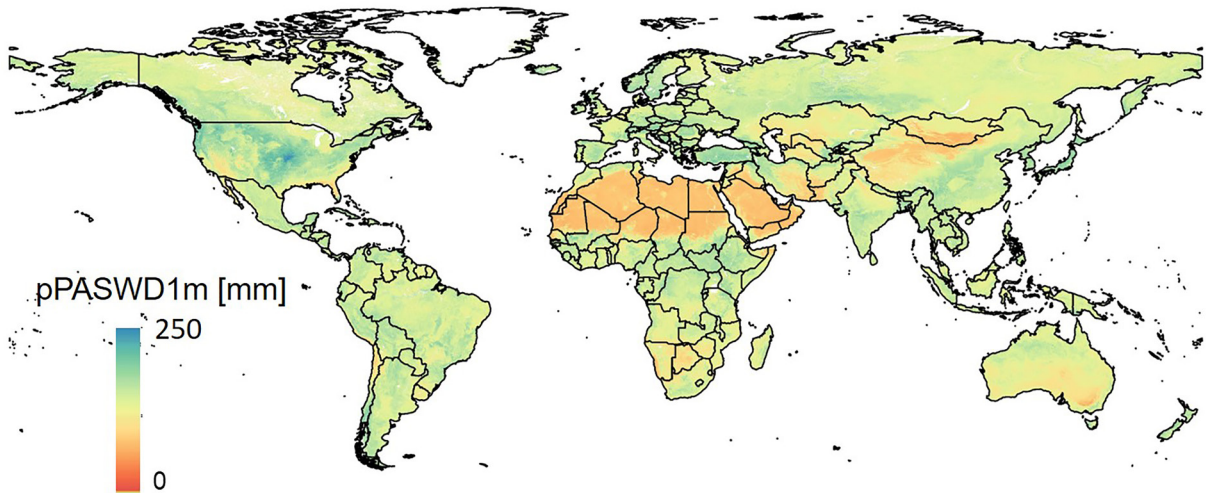
Climate regions	Field capacity (m <sup>3</sup> /m <sup>3</sup> )	Climatic water content (m <sup>3</sup> /m <sup>3</sup> )	Plant-available soil water (mm/1 m)	
			Potential	climatic
Tropical	0.30	0.29	154	140
Temperate	0.28	0.26	159	142
Arid	0.22	0.14	123	53
Boreal	0.23	0.20	151	119
Polar	0.23	0.20	145	114

## 4. Discussion

### 4.1. Effects of FC Definition on PASW

Using a definition of FC based on cessation of capillary flow (Figures 3 and 4) shows that most soils attain FC at matric potential values higher than  $-3.3$  m and water content values higher than traditional FC estimates. Consequently, global estimates of FC (and pPASW) based on this limit are expected to be higher as shown in Figure 6a. The dynamic definition of FC considering the time to attain negligible fluxes from leaky soils, provides a reasonable value of available water useable for plant uptake. The main difference between pPASWD1m and cPASWD1m (i.e., the height of PASW in first meter of soil) is observed in the arid region and shows that the primary driver to define cPASWD1m is whether rainfall events are frequent enough to replenish PASW. In tropical regions, the difference between pPASWD1m and cPASWD1m is minimal due to large and frequent rainfall, however, the soil

### a) Potential PASW



### b) Zhang et al., 2018

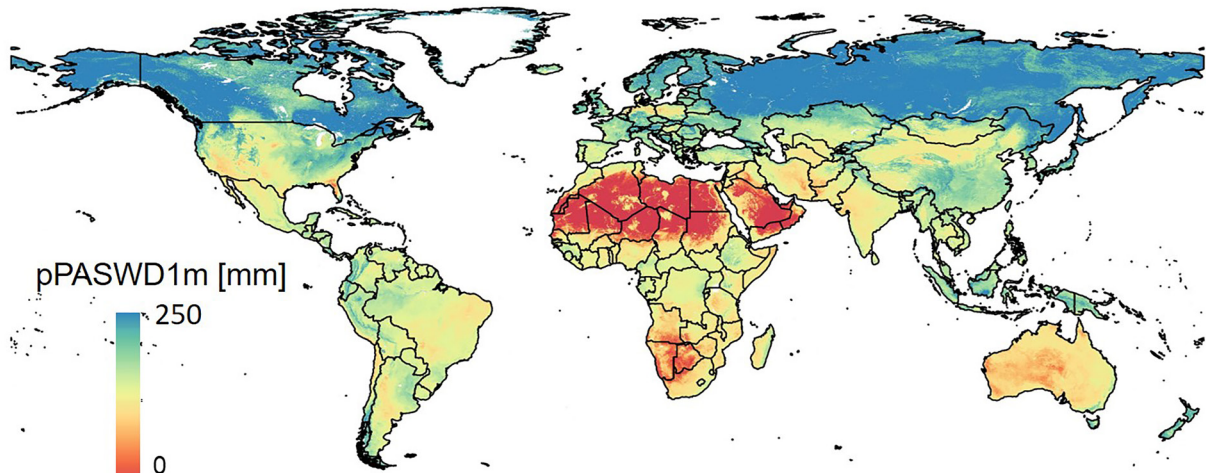
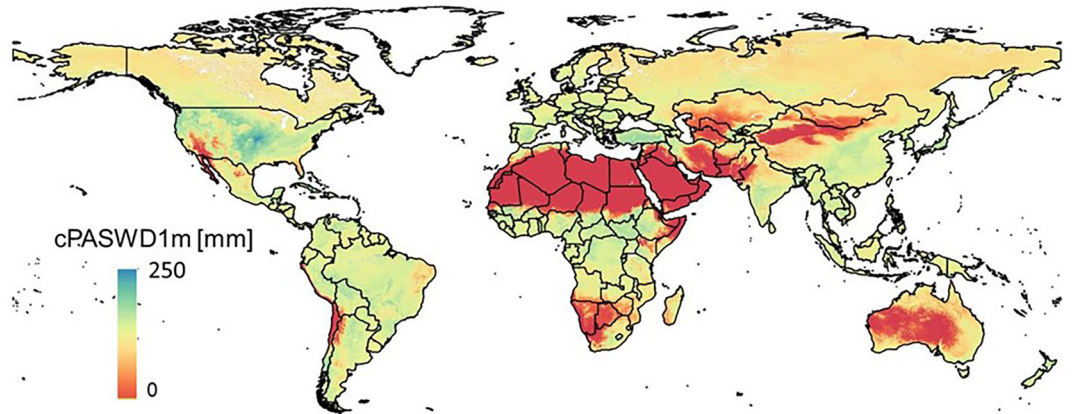


**Figure 7.** Comparison of global distribution of pPASWD1m (depth of plant available water in top meter of soil) computed (a) using Equation 8 with (b) the plant-available soil water map of Zhang et al. (2018).

a) Climatic PASW



b) Histogram pPASWD1m and cPASWD1m

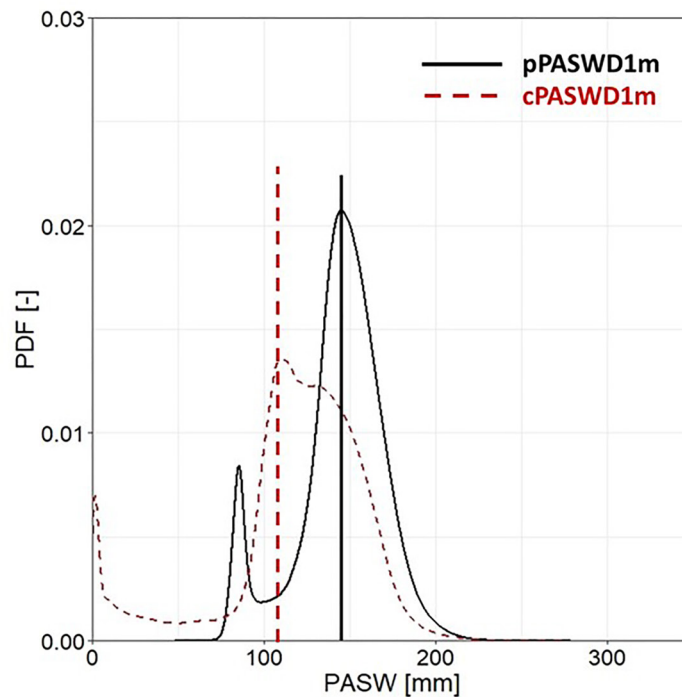


**Figure 8.** (a) Global and spatial distribution of climatically averaged plant-available soil water (PASW) taking into account evaporation losses in dry regions (reducing plant-available water); (b) statistical distribution of potential and climatic height of PASW in 1 m soil (pPASWD1m and cPASWD1m). Vertical lines represent mean PASW values (mean pPASWD1m = 144 mm and cPASWD1m = 107 mm). Note that, in order to plot the global probability distribution function of cPASW1m, the zero values from arid regions are not included to avoid the long peak at zero value.

structure and biopores in the soil may increase drainage and reduce runoff (Fatichi et al., 2020; Or, 2020) affecting vegetation growth that can be inhibited because of insufficient soil aeration and water flux (Turek et al., 2021).

#### 4.2. Potential and Climatic PASW

The concept of PASW has been used in agriculture for sizing irrigation systems to replenish the soil profile at peak water demand during a growing season (Lamm et al., 1994). Sandy soils require more frequent irrigation than silty soils with larger PASW storage capacity. For natural systems, the concept of PASW has been used in ecological studies (Liu et al., 2009; Randall et al., 2020) to investigate how soil modulates climatic inputs or forcing affecting



vegetation. In other words, PASW is not used for “design” or crop selection, but for interpretation of natural vegetation response to climatic conditions or changes in rainfall patterns. Nevertheless, as Koster and Suarez (2001) and Seneviratne et al. (2010) and many others have shown, PASW is a dominant factor in understanding climate memory and surface fluxes at intervals between rainfall events. More recently, PASW and vegetation received renewed interest in the context of the onset of continental heatwaves (Miralles et al., 2014; Seneviratne et al., 2010; Teuling et al., 2010). To supplement the traditional (agronomic) definition of PASW, it can be modified using local climate and identify regions where soil water content is persistently at or higher than FC and regions where water content is below FC. The climatic averaged plant available soil water (cPASW) introduced in this study delineates a realistic soil water storage picture that, in many regions, is significantly different from the standard definition of PASW (here denoted as potential plant available soil water, pPASW). The maps of cPASW and pPASW reconcile soil and climatic conditions concerning water storage available for vegetation. Note that the incorporation of climatic conditions affects arid climatic regions more compared to other climatic regions. We added the climatic mean annual potential evaporation losses to estimate the cPASW, which might be useful to provide a clear picture of the present climate. However, the recalculations of these maps will depend upon the rate of the change in the climate in the future.

### 4.3. Comparison of PASW Maps With Other Available Products

Figure 6 illustrates the comparison between the FC map derived using Assouline and Or (2014) approach and the map by Zhang et al. (2018) that used the standard definition of FC (−3.3 m head). Similarly, Figure 7 shows the comparison between (potential) PASW maps. We noticed the high values in central parts of India, the eastern parts of the USA, and parts of China, as compared to Zhang et al. (2018) PASW map. It is likely due to the presence of soils rich in smectite clay minerals that reduce the soil permeability and increase soil specific surface area thus enhancing the water storage capacity. Zade et al. (2020) also discussed the dominant role of smectite clay minerals on agriculture in central India and their effect on PASW (which is always high as compared to other soil types). Moreover, in the new maps the tropical region's soil has more water and the higher northern latitudes soil have less water as compared to Zhang et al. (2018) PASW map. This might be the effect of the parameterization of SWCC used for these regions or the definition of FC itself. There are other global and regional maps of PASW products published in the last decade. For example, Kleidon (2011) estimated the total PASW storage capacity of the rooting zone depth for the whole globe on a 1.0° grid using inverse modeling. Similarly, Leenaars et al. (2018) developed the PASW map for south Africa by subtracting the FC (considered water content at three matric potentials −1, −2, and −3 m for coarse, intermediate and fine textures, respectively) with WP (−150 m matric potential). Kristensen et al. (2019) developed the PASW at 1 m for Europe using the standard approach and considered the FC at −1 m matric potential. We could not compare these studies with our map because most of the maps calculated the PASW considering plant rooting depth that can be different from the 1 m depth PASW map. Kristensen et al. (2019) calculated the PASW for 1 m soil depth but the maps are not publicly available. The major addition in our study is that we consider the climatic effect on PASW while the other studies focused on pPASW.

### 4.4. Use of Field Capacity and Plant Available Soil Water Maps

The primary advantage of FC maps is estimating the amount of water available for plants. The PASW map can be used as an input in crop models to describe water uptake and transpiration (Brisson et al., 2003). The drought intensity in agriculture and forest can also be computed using these maps (Meusburger et al., 2022). The land surface models also need PASW as an input to simulate land-atmosphere coupling responses (Shrestha & Simmer, 2019). Besides this, the modified maps could improve the predictions in all applications because the hydraulic parameters ( $\alpha$ ,  $n$ ,  $\theta_s$ , and  $\theta_r$ ) are not derived using PTFs. The actual soil water characteristics curves fitted parameters were utilized to develop these maps. Moreover, the FC was not considered at particular matric potential. It was estimated based on the approach of Assouline and Or (2014) and reflects soil intrinsic properties. Furthermore, the pPASW maps can overestimate the predictions for arid regions, while the cPASW map could be employed for a more accurate representation in such areas.

### 4.5. Limitations of the Study

Some limitations need to be taken into account while using these maps. The pPASW and cPASW define the potential and cPASW for 1 m depth. We ignored the depth of bedrock and impermeable layers in our calculations. However, only 7% of the terrestrial area has soil thickness of less than 1 m particularly at high elevations

(computed using Pelletier et al. (2016) data set). Moreover, we assumed soil reaches saturation after each rainfall event and then start counting the days to attain FC. However, the rainfall amounts are not always enough for the soil to become fully saturated. Also, the vegetative growth, root water take, and bio-pores are not taken into account while calculating the days to attain FC. Lastly, the role of runoff is also missing. Despite these limitations, our maps can be used in various applications as mentioned above.

## 5. Conclusion

We provide the state-of-the-art spatial distribution and parameters for PASW in terms of soil properties (pPASW) and link the potential water storage with climatic conditions (cPASW). Globally, ice-free soils store up to 19,941 km<sup>3</sup> of water in the top 1 m representing about 18% of the annual terrestrial precipitation (111,000 km<sup>3</sup>/yr; Oki and Kanae (2006)). Adjusted for local climatic conditions, PASW global storage rarely exceeds 14,853 km<sup>3</sup> per year. The global storage and spatial distribution of PASW highlight the need for multiple refilling events of soil profiles. The limited storage capacity also reflects the leaky nature of the soil reservoir that is strongly coupled with vegetation that continuously transpires this temporary storage back to the atmosphere. Hence, PASW reflects a dynamic soil water reservoir whose magnitude varies with soil type and climatic region. In arid regions, this reservoir is never filled with enough water for vegetation cover and physiology. Even in tropical regions that are expected to maintain water content above FC due to large and frequent rainfall, soil structure and biopores act to drain the profile such as that unsaturated conditions essential for soil aeration are rapidly restored.

## Notation

PASW	is the plant available soil water content, difference between FC and WP
PASWD	is the plant available soil water height within certain soil depth, dimension of length.
PASWD1m	is the plant available soil water height in the first meter of soil, dimension of mm water per <i>m</i> of soil
PASWV	is the plant available soil water volume in a certain soil volume, dimension of length <sup>3</sup> .
PASWV1m	is the plant available soil water volume in a soil volume of 1 m depth, dimension of length <sup>3</sup> per <i>m</i> soil depth

## Data Availability Statement

The data sets produced in this study are available at <https://doi.org/10.5281/zenodo.6777125> (Gupta et al., 2022).

## References

- Asadi, Z., Mohammadi, M., Shorafa, M., Farhbakhsh, M., & Ghezlbas, E. (2020). Evaluation of Assouline–or adjusted model to express soil drainage curve. *Eurasian Soil Science*, 53(6), 749–759. <https://doi.org/10.1134/s1064229320060022>
- Assouline, S., & Or, D. (2014). The concept of field capacity revisited: Defining intrinsic static and dynamic criteria for soil internal drainage dynamics. *Water Resources Research*, 50(6), 4787–4802. <https://doi.org/10.1002/2014wr015475>
- Beck, H. E., Wood, E. F., Pan, M., Fisher, C. K., Miralles, D. G., Van Dijk, A. I., et al. (2019). MSWEP V2 global 3-hourly 0.1 precipitation: Methodology and quantitative assessment. *Bulletin of the American Meteorological Society*, 100(3), 473–500. <https://doi.org/10.1175/bams-d-17-0138.1>
- Bickel, S., & Or, D. (2020). Soil bacterial diversity mediated by microscale aqueous-phase processes across biomes. *Nature Communications*, 11(1), 1–9. <https://doi.org/10.1038/s41467-019-13966-w>
- Bickel, S., & Or, D. (2021). *Dataset of global climatic soil water contents and consecutive dry days*. Zenodo. <https://doi.org/10.5281/zenodo.5078258>
- Brisson, N., Gary, C., Justes, E., Roche, R., Mary, B., Ripoche, D., et al. (2003). An overview of the crop model STICS. *European Journal of Agronomy*, 18(3–4), 309–332. [https://doi.org/10.1016/s1161-0301\(02\)00110-7](https://doi.org/10.1016/s1161-0301(02)00110-7)
- Colman, E. (1947). A laboratory procedure for determining the field capacity of soils. *Soil Science*, 63(4), 277–284. <https://doi.org/10.1097/00010694-194704000-00003>
- Dahiya, I., Dahiya, D., Kuhad, M., & Karwasra, S. (1988). Statistical equations for estimating field capacity, wilting point and available water capacity of soils from their saturation percentage. *The Journal of Agricultural Science*, 110(3), 515–520. <https://doi.org/10.1017/s0021859600082083>
- Dai, Y., Xin, Q., Wei, N., Zhang, Y., Shangguan, W., Yuan, H., et al. (2019). A global high-resolution dataset of soil hydraulic and thermal properties for land surface modeling. *Journal of Advances in Modeling Earth Systems*, 11(9), 2996–3023. <https://doi.org/10.1029/2019ms001784>
- de Jong van Lier, Q., & Wendroth, O. (2016). Reexamination of the field capacity concept in a Brazilian Oxisol. *Soil Science Society of America Journal*, 80(2), 264–274. <https://doi.org/10.2136/sssaj2015.01.0035>
- Fatihchi, S., Or, D., Walko, R., Vereecken, H., Young, M. H., Ghezzehei, T. A., et al. (2020). Soil structure is an important omission in Earth System Models. *Nature Communications*, 11(1), 1–11. <https://doi.org/10.1038/s41467-020-14411-z>

## Acknowledgments

The study was supported by ETH Zurich (Grant ETH-18 18-1). We would like to thank the anonymous reviewers and editor, their comments greatly improved the manuscript.

- Fick, S. E., & Hijmans, R. J. (2017). WorldClim 2: New 1-km spatial resolution climate surfaces for global land areas. *International Journal of Climatology*, 37(12), 4302–4315. <https://doi.org/10.1002/joc.5086>
- Gupta, S., Lehmann, P., Bickel, S., Bonetti, S., & Or, D. (2022). *Global maps of potential and climatic plant-available soil water*. Zenodo. <https://doi.org/10.5281/zenodo.6777125>
- Gupta, S., Lehmann, P., Bonetti, S., Papritz, A., & Or, D. (2021). Global prediction of soil saturated hydraulic conductivity using random forest in a covariate-based geotransfer function (CoGTF) framework. *Journal of Advances in Modeling Earth Systems*, 13(4), e2020MS002242. <https://doi.org/10.1029/2020ms002242>
- Gupta, S., Papritz, A., Lehmann, P., Hengl, T., Bonetti, S., & Or, D. (2022a). Global mapping of soil water characteristics parameters; fusing curated data with machine learning and environmental covariates. *Remote Sensing*, 14(8), 1947. <https://doi.org/10.3390/rs14081947>
- Gupta, S., Papritz, A., Lehmann, P., Hengl, T., Bonetti, S., & Or, D. (2022b). Global soil hydraulic properties dataset based on legacy site observations and robust parameterization. *Scientific Data*, 9(1), 444. <https://doi.org/10.1038/s41597-022-01481-5>
- Hillel, D. (2012). *Soil and water: Physical principles and processes*. Elsevier.
- Jabro, J., Evans, R., Kim, Y., & Iversen, W. (2009). Estimating in situ soil–water retention and field water capacity in two contrasting soil textures. *Irrigation Science*, 27(3), 223–229. <https://doi.org/10.1007/s00271-008-0137-9>
- Jensen, M. E., & Haise, H. R. (1963). Estimating evapotranspiration from solar radiation. *Journal of the Irrigation and Drainage Division*, 89(4), 15–41. <https://doi.org/10.1061/jrcea4.0000287>
- Kirkham, M. (2005). *Principles of soil and plant water relations* Elsevier.
- Kleidon, A. (2011). *ISLSCP II total plant-available soil water storage capacity of the rooting zone*. ORNL Distributed Active Archive Center. <https://doi.org/10.3334/ORNLDAAAC/1006>
- Koster, R. D., & Suarez, M. J. (2001). Soil moisture memory in climate models. *Journal of Hydrometeorology*, 2(6), 558–570. [https://doi.org/10.1175/1525-7541\(2001\)002<0558:smmicm>2.0.co;2](https://doi.org/10.1175/1525-7541(2001)002<0558:smmicm>2.0.co;2)
- Kosugi, K. (1994). Three-parameter lognormal distribution model for soil water retention. *Water Resources Research*, 30(4), 891–901. <https://doi.org/10.1029/93wr02931>
- Kristensen, J. A., Balstrøm, T., Jones, R. J., Jones, A., Montanarella, L., Panagos, P., & Breuning-Madsen, H. (2019). Development of a harmonised soil profile analytical database for Europe: A resource for supporting regional soil management. *Soil*, 5(2), 289–301. <https://doi.org/10.5194/soil-5-289-2019>
- Lamm, F., Rogers, D., & Manges, H. (1994). Irrigation scheduling with planned soil water depletion. *Transactions of the ASAE*, 37(5), 1491–1497. <https://doi.org/10.13031/2013.28232>
- Leenaars, J. G., Claessens, L., Heuvelink, G. B., Hengl, T., González, M. R., van Bussel, L. G., et al. (2018). Mapping rootable depth and root zone plant-available water holding capacity of the soil of sub-Saharan Africa. *Geoderma*, 324, 18–36. <https://doi.org/10.1016/j.geoderma.2018.02.046>
- Lehmann, P., Assouline, S., & Or, D. (2008). Characteristic lengths affecting evaporative drying of porous media. *Physical Review E*, 77(5), 056309. <https://doi.org/10.1103/physreve.77.056309>
- Liu, W., Zhang, Z., & Wan, S. (2009). Predominant role of water in regulating soil and microbial respiration and their responses to climate change in a semiarid grassland. *Global Change Biology*, 15(1), 184–195. <https://doi.org/10.1111/j.1365-2486.2008.01728.x>
- Logsdon, S. (2019). Should upper limit of available water be based on field capacity? *Agrosystems, Geosciences & Environment*, 2(1), 1–6. <https://doi.org/10.2134/age2019.08.0066>
- Mantovanelli, B. C., Petry, M. T., Weiler, E. B., & Carlesso, R. (2021). Geostatistical interpolation based ternary diagrams for estimating water retention properties in soils in the center-south regions of Brazil. *Soil and Tillage Research*, 209, 104973. <https://doi.org/10.1016/j.still.2021.104973>
- Meusbürger, K., Trotsiuk, V., Schmidt-Walter, P., Baltensweiler, A., Brun, P., Bernhard, F., et al. (2022). Soil–plant interactions modulated water availability of Swiss forests during the 2015 and 2018 droughts. *Global Change Biology*, 28(20), 5928–5944. <https://doi.org/10.1111/gcb.16332>
- Minasny, B., & McBratney, A. (2018). Limited effect of organic matter on soil available water capacity. *European Journal of Soil Science*, 69(1), 39–47. <https://doi.org/10.1111/ejss.12475>
- Miralles, D. G., Teuling, A. J., Van Heerwaarden, C. C., & Vilà-Guerau de Arellano, J. (2014). Mega-heatwave temperatures due to combined soil desiccation and atmospheric heat accumulation. *Nature Geoscience*, 7(5), 345–349. <https://doi.org/10.1038/ngeo2141>
- Mualem, Y. (1976). A new model for predicting the hydraulic conductivity of unsaturated porous media. *Water Resources Research*, 12(3), 513–522. <https://doi.org/10.1029/wr012i003p00513>
- Oki, T., & Kanae, S. (2006). Global hydrological cycles and world water resources. *Science*, 313(5790), 1068–1072. <https://doi.org/10.1126/science.1128845>
- Or, D. (2020). The tyranny of small scales—On representing soil processes in global land surface models. *Water Resources Research*, 56(6). <https://doi.org/10.1029/2019WR024846>
- Otoni Filho, T. B., Otoni, M. V., Oliveira, M. B. D., Macedo, J. R. D., & Reichardt, K. (2014). Revisiting field capacity (FC): Variation of definition of FC and its estimation from pedotransfer functions. *Revista Brasileira de Ciência do Solo*, 38(6), 1750–1764. <https://doi.org/10.1590/s0100-06832014000600010>
- Pelletier, J. D., Broxton, P. D., Hazenberg, P., Zeng, X., Troch, P. A., Niu, G.-Y., et al. (2016). A gridded global data set of soil, intact regolith, and sedimentary deposit thicknesses for regional and global land surface modeling. *Journal of Advances in Modeling Earth Systems*, 8(1), 41–65. <https://doi.org/10.1002/2015ms000526>
- Randall, K. C., Brennan, F., Clipson, N., Creamer, R. E., Griffiths, B. S., Storey, S., & Doyle, E. (2020). An assessment of climate induced increase in soil water availability for soil bacterial communities exposed to long-term differential phosphorus fertilization. *Frontiers in Microbiology*, 11, 682. <https://doi.org/10.3389/fmicb.2020.00682>
- Robertson, B. B., Almond, P. C., Carrick, S. T., Penny, V., Chau, H. W., & Smith, C. M. (2021). Variation in matric potential at field capacity in stony soils of fluvial and alluvial fans. *Geoderma*, 392, 114978. <https://doi.org/10.1016/j.geoderma.2021.114978>
- Seneviratne, S. I., Corti, T., Davin, E. L., Hirschi, M., Jaeger, E. B., Lehner, I., et al. (2010). Investigating soil moisture–climate interactions in a changing climate: A review. *Earth-Science Reviews*, 99(3–4), 125–161. <https://doi.org/10.1016/j.earscirev.2010.02.004>
- Shrestha, P., & Simmer, C. (2019). Modeled land atmosphere coupling response to soil moisture changes with different generations of land surface models. *Water*, 12(1), 46. <https://doi.org/10.3390/w12010046>
- Silva, B. M., Silva, É. A. D., Oliveira, G. C. D., Ferreira, M. M., & Serafim, M. E. (2014). Plant-available soil water capacity: Estimation methods and implications. *Revista Brasileira de Ciência do Solo*, 38(2), 464–475. <https://doi.org/10.1590/s0100-06832014000200011>
- Simons, G., Koster, R., & Droogers, P. (2020). Hihydrosoil v2. 0-high resolution soil maps of global hydraulic properties. Retrieved from <https://www.futurewater.nl/wp-content/uploads/2020/10/HiHydroSoil-v2.0-High-Resolution-Soil-Maps-of-Global-Hydraulic-Properties.pdf>

- SSSA. (2008). *Glossary of soil science terms 2008*. ASA-CSSA-SSSA.
- Teuling, A. J., Seneviratne, S. I., Stöckli, R., Reichstein, M., Moors, E., Ciais, P., et al. (2010). Contrasting response of European forest and grassland energy exchange to heatwaves. *Nature Geoscience*, 3(10), 722–727. <https://doi.org/10.1038/ngeo950>
- Turek, M. E., Armindo, R. A., & Wendroth, O. (2021). Hydraulic energy indices reveal spatial dependence in a subtropical soil under maize crop in Southern Brazil. *Pedosphere*, 31(5), 771–782. [https://doi.org/10.1016/s1002-0160\(20\)60093-5](https://doi.org/10.1016/s1002-0160(20)60093-5)
- Twarakavi, N. K., Sakai, M., & Simunek, J. (2009). An objective analysis of the dynamic nature of field capacity. *Water Resources Research*, 45(10), W10410. <https://doi.org/10.1029/2009wr007944>
- van Genuchten, M. T. (1980). A closed-form equation for predicting the hydraulic conductivity of unsaturated soils. *Soil Science Society of America*, 44(5), 892–898. <https://doi.org/10.2136/sssaj1980.03615995004400050002x>
- Veihmeyer, F., & Hendrickson, A. (1931). The moisture equivalent as a measure of the field capacity of soils. *Soil Science*, 32(3), 181–194. <https://doi.org/10.1097/00010694-193109000-00003>
- Veihmeyer, F., & Hendrickson, A. (1949). Methods of measuring field capacity and permanent wilting percentage of soils. *Soil Science*, 68(1), 75–94. <https://doi.org/10.1097/00010694-194907000-00007>
- Wheeler, D., & Read, C. (2016). Spotlight on overseer: Perspectives and approaches to addressing nutrient management challenges using an integrated farm systems model. In *International nitrogen initiative conference*.
- Zacharias, S., & Bohne, K. (2008). Attempt of a flux-based evaluation of field capacity. *Journal of Plant Nutrition and Soil Science*, 171(3), 399–408. <https://doi.org/10.1002/jpln.200625168>
- Zade, S., Vaidya, P., Kadu, P., & Tiwary, P. (2020). Plant available water capacity (PAWC) for deep-rooted crops in cracking clay soils (Vertisols) of semi-arid Central India. *Clay Research*, 39(2), 89–109. <https://doi.org/10.5958/0974-4509.2020.00010.8>
- Zhang, Y., & Schaap, M. G. (2017). Weighted recalibration of the Rosetta pedotransfer model with improved estimates of hydraulic parameter distributions and summary statistics (Rosetta3). *Journal of Hydrology*, 547, 39–53. <https://doi.org/10.1016/j.jhydrol.2017.01.004>
- Zhang, Y., Schaap, M. G., & Zha, Y. (2018). A high-resolution global map of soil hydraulic properties produced by a hierarchical parameterization of a physically based water retention model. *Water Resources Research*, 54(12), 9774–9790. <https://doi.org/10.1029/2018wr023539>